

A facile plant-mediated green synthesis of Magnesium oxide nanoparticles by combustion method using *Terminalia Chebula* seed and their applications in the synthesis of selenoesters and biodiesel from used cooking oil

H. S. Lalithamba^{*1}, Omkaresh B. R.^{*2}, Aisha Siddekha³, K. V. Anusuya³

^{*1}Department of Chemistry, Siddaganga Institute of Technology, B.H. Road, Tumakuru-572 103, Karnataka, India. Mail: hsl@sit.ac.in +919008305654

^{*2}Department of Mechanical Engineering, Siddaganga Institute of Technology, B.H. Road, Tumakuru-572 103, Karnataka, India. Mail: omkar@sit.ac.in

³Department of Chemistry, Government First Grade College, B.H. Road, Tumakuru-572 102, Karnataka, India.

Abstract:

Synthesis of magnesium oxide nanoparticles (MgO NPs) using *Terminalia chebula* seeds extract as fuel by solution combustion method and their applications have been reported in this study. Characterization of the synthesized MgO NPs via Powder XRD, FT-IR, SEM, TEM and EDAX for structural and morphological studies was carried out. MgO NPs were used as a catalyst for production of biodiesel from used cooking oil and for the synthesis of selenoesters. The selenoesters were analyzed by mass spectrometry, ¹H NMR, ¹³C NMR, FTIR techniques and the antifungal activity was investigated for some of the selenoesters against two pathogenic strains *F. oxysporum* and *A. niger* with Fluconazole as a standard drug. Biodiesel produced was tested for conformity with the ASTM standard and the results are reported herein. This is one of the novel methods reported for the synthesis of MgO NPs using *terminalia chebula* seeds, which are easily available, non-toxic, make the NPs green. Catalytic performance of these MgO NPs can be explored further for the synthesis of other organic compounds.

Key words: MgO NPs; *Terminalia chebula*; Combustion method; Selenoesters; Antifungal activities; Biodiesel

Abbreviations

PXRD	Powder X-ray diffraction
UV–visible	Ultraviolet–visible spectroscopy
BET	Brunauer–Emmett–Teller
CuO NPs	Copper oxide nanoparticles
TBME	<i>Terminalia Billerica</i> Methyl ester
FTIR	Fourier transform infrared spectroscopy
SEM	Scanning electron microscopy
Ea	Activation energy
MgO NPs	Magnesium oxide Nano Particles
BJH	Barrett–Joyner–Halenda
¹ H NMR	Proton Nuclear Magnetic Resonance Spectroscopy
¹³ C NMR	Carbon-13 Nuclear Magnetic Resonance Spectroscopy
DMSO	Dimethylsulphoxide
TLC	Thin-layer chromatography
FFA	Free fatty acids
JCPDS	Joint Committee on Powder Diffraction Standards
HPLC	High-performance liquid chromatography
R	Universal gas constant (8.314 J mol ^{−1} K ^{−1})
ASTM	American Society for Testing and Materials

1. Introduction

Nanoparticles have earned special attention for being useful to chemists in the laboratory as well as in the industry as wonderful catalysts owing to their property of activation of adsorbed compounds and improving the reaction rates, high selectivity, environment-friendly nature, and easier work-up. Nano-structured materials in comparison with the micron-sized materials have a characteristic large specific surface areas exposing large fraction of atoms available for chemical reaction. Hence many nano particles such as nano MgO, ZnO, CuO, CeO₂ etc., have been used as catalysts[1-2] or as reagents. magnesium oxide nanoparticles (MgO NPs) have served as a catalyst as well as reagent owing to their improved chemical and physical properties in many syntheses. Industrial applications of MgO NPs as adsorbents, defluorination of water during purification, catalysis, additive to heavy fuel oils, medical sciences, lithium-ion batteries, and biosensors *etc.* have been explored.[3] To prepare MgO NPs many methods have been employed such as precipitation, carbothermic reduction, sonochemical, solvothermal, microwave irradiations and thermal decomposition of precursors *etc.* as revealed by the literature survey. Chemical methods of synthesis of the nanoparticles lead to the adsorption of certain toxic chemicals on the surface of NPs which may lead to adverse effects, hence not

suitable for medical applications. In the recent past with the advent of green chemistry principles, cleaner and greener syntheses have garnered the attention of researchers and there are reports of syntheses of plant based nanoparticles.[4] Plant-mediated metal oxide nanoparticles have contributed significantly for the greener organic synthesis as heterogeneous catalysts, reagents as bioengineering materials etc. offering the advantages of low cost, increased efficiency, and are easy on the environment.[5] Literature survey reveals the green synthesis of different NPs using plant extracts of black tea,[6] neem, [7] papaya,[8] tamarind,[9] and alfalfa[10] have been reported. A recent review reports the synthesis and application of MgO NPs in organic transformations, using plant extracts, which provide the reducing or stabilizing agents required for the NPs synthesis with a suitable metal salt such as nitrates, chlorides or acetates of metals as precursors.[11] *Terminalia chebula* (Myrobalan) is a rich source of phenolic and flavonoid compounds and shows antioxidant, anticholinesterase inhibitory, and antimicrobial activities.[12] In continuation of our research on synthesis of heterogeneous metal NPs catalysts and their synthetic applications,[13] a novel protocol for the facile green synthesis of MgO NPs using these *Terminalia chebula* seed extract *via* solution combustion method has been reported in this study.

Selenium is a micronutrient responsible for biochemical processes which play pivotal role in maintaining human health.[14] Selenium is found in oxido-reductase enzymes such as dehydrogenases, glutathione peroxidase, hydrogenases.[15] These enzymes contain amino acids- selenomethionine and selenocysteine; and are responsible for antioxidant, anticancer and anti-inflammation activity in the human body.[16-17] Diselenides are the first organoselenium compounds to be synthesized.[18] Selenides and diselenides are employed as flexible starting materials for various functional group transformations, as these are stable but sufficiently reactive to produce many electrophilic, nucleophilic and radicophilic species.[19] Several transformations can be brought about as selenols, selenides, selenoxides, selenones, halides, selenocyanates, selenenic acids and their esters. Selenides and diselenides find use as prooxidant, anticancer, cytotoxic and radioprotective[20-22]agents. With the increasing incidences of cancer and related diseases, there is a growing need for the development of potent anticancer reagents. In general, organoselenium compounds are proving to be good chemo preventive agents compared to their inorganic variants.[23] Inorganic diselenides find use in spectrometers, detectors, accelerators, and solar cells.[24-26] Due to their unique redox

properties they also play important role as catalysts in organic transformations such as 1, 4-addition of Grignard reagents to enones,[27] asymmetric allylic substitution,[28] and asymmetric hydrosilylation.[29] Among the organoselenium compounds, selenoesters find use as liquid crystals of nematic type,[30] in native chemical ligation (NCL) reactions[31] and alkaloids.[32] These selenium compounds reportedly exhibit antioxidant,[33] cytotoxic and antiproliferative activities.[34-35] Further, selenoesters are powerful tools in synthetic organic chemistry, useful as acyl-transfer reagents, [36] protecting groups[37] and in synthesis of natural products.[38] Reports reveal that the anti-cancer activity is determined by the chemical forms and dose of selenium. Bioavailability of selenoesters compared to inorganic selenium compounds makes them more potent anti-cancer agents.[39-40]

Many approaches have been reported in the past for the synthesis of selenoesters; Owing to their broad-spectrum biological activities, new protocols with improvised syntheses of selenoesters are still being reported. These compounds have been synthesized, from Diorganyl diselenides and acyl chlorides using microwave irradiation,[41] from aldehydes employing *i*-Bu₂AlSeR,[42] SeCO,[43] and Hg (SePh)₂.[44] Synthesis of selenoesters from α -amino carbonyl and glycine derivatives using Iron (III) and zinc catalyst have also been reported (**Scheme 1**).[45-49]. Recent study on phenyl selenoesters synthesis from anhydrides in metal free reaction condition has been reported.[47]

Continuing our efforts in the synthesis of varieties peptidomimetic molecules using various nano metal oxides, this study also intended to explore the catalytic activity of MgO NPs towards the synthesis of selenoesters derivatives of N^α -protected amino acids by coupling of sodium selenoate and α -bromoester. Literature survey reveals many metal oxide NPs being synthesized using extracts of different parts of several plants and their characterization being reported. Research gaps identified in this regard include the need to investigate the role of MgO NPs as catalysts in organic synthesis. Therefore, the investigation of catalytic performance of MgO NPs for the synthesis of N^α -protected selenoesters was taken up. Reuse of used cooking oil for biodiesel production holds the potential to upgrade it to higher production range from the laboratory scale. The present study reports the facile synthesis, characterization, and applications of MgO NPs, as well as the characterization and antifungal activity of synthesized N^α -protected selenoesters employing Fluconazole as a reference standard.

2. Experimental section

2.1 Materials and methodology

All chemicals were purchased from Sigma-Aldrich and Merck and used as obtained without any further purification. Seeds of *Terminalia Chebula* were obtained from Banneraghatta forest, Karnataka, (India). Powder XRD was recorded on Shimadzu make X-ray diffractometer (PXRD-7000) using Cu-K α radiation of wavelength $\lambda = 1.541 \text{ \AA}$. IR spectra were determined on Bruker Alpha-T FTIR spectrometer. Melting points were determined using capillary method using melting point apparatus. ^1H NMR and ^{13}C NMR spectra were conducted on Bruker AMX 400 MHz spectrometer using TMS and CDCl_3 / DMSO as solvent. Mass spectral analyses were carried out on a Micromass Q-ToF Micro Mass Spectrometer.

2.2. Combustion synthesis of MgO NPs

Of the various methods used for the synthesis of metal NPs such as, sol-gel method, co-precipitation, solution combustion synthesis, spray method etc. solution combustion synthesis is a most widely used, efficient, rapid and cost-efficient method for the synthesis metal-based NPs.[48] Particle size and morphology of metal oxide NPs depends on parameters such as calcination temperature, pH, and different fuels used.[49] To begin with, *Terminalia Chebula* seeds were cleaned, dried and powdered. MgO NPs were prepared by combustion method[50] using *Terminalia Chebula* seed powder (as a fuel) and $\text{Mg}(\text{NO}_3)_2 \cdot 6\text{H}_2\text{O}$ (as source of magnesium). The reaction mixture was prepared by mixing *Terminalia Chebula* seed powder (10 g) and $\text{Mg}(\text{NO}_3)_2 \cdot 6\text{H}_2\text{O}$ (5g) in 15 mL of distilled water taken in a silica crucible and stirred for 3-5 minutes till a uniform solution was formed. This reaction mixture was heated in a pre-heated muffle furnace maintained at 450 °C. Within 30 minutes, MgO NPs were formed which were further calcined at 800 °C. The particles obtained were stored in a desiccator for further studies.

2.3. Synthetic route for N^α -protected selenoester using MgO NPs

To a suspension of selenium metal (1 g, 12.66 mmol) powder in distilled water, NaBH_4 solution (1g, 26.5 mmol in 12 mL of distilled H_2O) was added slowly. With the continued stirring colourless solution of NaHSe was formed. To this solution, N^α -protected amino acid chloride, Fmoc-valine (1.8 g, 12.8 mmol) was added at room temperature. To this catalytic amount

of MgO NPs (0.70 mmol) and α -bromoester (1.4 g, 13 mmol) were added with stirring for 5-10 minutes. Then, the reaction mixture was extracted into 20 mL of EtOAc and the catalyst was filtered off. The filtrate was washed with dil. HCl, Na₂CO₃, and brine solutions. Column chromatography using hexane-EtOAc (10:1) gives the pure products.

2.4. Study of antifungal activity selenoesters

Evaluation of antifungal activity was taken up for the selenoesters, using two pathogenic fungicidal strains *Fusarium oxysporum* [51] and *Aspergillus niger* [52] by cup-plate agar diffusion method. Holes were made using sterile cork borer in the agar and these were filled with 100 μ g/ μ L concentration using DMSO (dimethyl sulfoxide), fluconazole (25 μ g/ μ L) and after the incubation for 24h at 37°C the inhibition zones were measured (mm). Simultaneously, Fluconazole (standard) was tested against the pathogenic fungicidal strains.

2.5. Production of biodiesel

Production of biodiesel using used cooking oil *via* transesterification reaction with MgO NPs (1% w/v) as catalyst and methanol as solvent was carried out. After the completion of reaction (about 90 minutes), the process yields 90 % of biodiesel. The biodiesel obtained was tested as per ASTM standards.

3. Results and Discussion

3.1 Characterization of MgO NPs

3.1.1. X-Ray Diffraction analysis

To establish the crystalline structure of MgO NPs, XRD analysis was carried out (**Figure 1**). High crystallinity of the sample was indicated by the sharp diffraction lines. Presence of intense and sharp peaks at 37.0°, 42.92°, 62.28° corresponding to (111), (200) and (220) planes, respectively, indicated the formation of MgO NPs. The diffraction peaks matched with Joint Committee on Powder Diffraction Standards [JCPDS file: 45-0946].[53] The Debye-Scherrer's equation (i) was used to calculate the average crystallite size of the prepared sample.

$$D = \frac{K \lambda}{\beta \cos \theta} \quad \text{----- (i)}$$

where, D is crystalline size, K is Scherrer constant, λ is X-ray wavelength, β is full-width at half-maximum and θ is Bragg's angle. Debye Scherrer's calculations indicate the average crystallite size of MgO NPs to be 32.76 nm.

3.1.2. *Fourier Transform Infrared Spectroscopy*

Metal oxide bond stretching frequencies of the MgO NPs were analyzed by FT-IR. A prominent peak at $\nu = 440\text{ cm}^{-1}$ in the spectrum (**Figure 2**) can be ascribed to the stretching vibrations of Mg–O bonds. The peak observed at 1645 cm^{-1} is for carbonyl group and the presence of –OH stretching is observed at 3435 cm^{-1} indicating water adsorption on the surface of metal oxide. The peak at 1114 cm^{-1} can be attributed to the C–O stretch of either the phenolic or flavonoids from the plant extract.

3.1.3. *Scanning Electron Microscopy analysis*

To establish the particle size and morphology of MgO NPs, the SEM images are presented in **Figure 3**. Clusters with bead-like morphology (**Figure 3a**) of pure MgO NPs calcined at 800°C are indicated. The voids present (**Figure 3b**) indicate the evolution of gaseous elements during the synthesis.

3.1.4. *Energy dispersive analysis of X-ray*

The EDAX spectrum (**Figure 4**) of MgO NPs sample shows the existence of Mg and O at appropriate concentrations. The atomic % of Mg and O element in MgO is found to be 42.85 and 56.26, respectively and shows the stoichiometric relationship (1:1) between magnesium and oxygen.

3.1.5. *Transmission Electron Microscopy analysis*

TEM images give valuable information regarding the shape, mean particle size and particle size distribution of nanoparticles. The TEM images (**Figure 5a** magnification 100kX and **Figure 5b** magnification 50kX) point to the spherical shape of synthesized MgO NPs having a size of approximately 10-30 nm.

3.1.6. *UV-Visible analysis of MgO NPs*

Figure 6a gives the diffuse reflectance spectrum (DRS) of MgO NPs taken at room temperature. Characteristic excitonic absorption peak of MgO particles was observed at around 400 nm. The diffused spectrum is represented in **Figure 6b** and the calculated band gap is 5.28 eV. Energy gap difference observed is very small which can be attributed to synthesis method, particle size, crystallinity, and morphology.

3.2. *Synthesis of N^{α} -protected selenoester using MgO NPs*

In order to develop a facile route for the preparation of selenoesters (**Scheme 2**) to establish the

catalytic performance of MgO NPs, a model reaction was carried out. To a suspension of selenium metal (1 g, 12.66 mmol) powder in distilled water, NaBH₄ solution (1g, 26.5 mmol in 12 mL of distilled H₂O) was added slowly. A vigorous reaction takes place with the evolution of H₂ and heat. A colorless solution of NaHSe was formed with the continued stirring. To this solution, *N*^α-protected amino acid chloride, Fmoc-valine (1.8 g, 12.8 mmol) was added at room temperature. Sodium selenoate of the protected amino acid was obtained as a reddish-brown colored solution. To this catalytic amount of MgO NPs (0.75 mmol) and α-bromoester (1.4 g, 13 mmol) were added while stirring for 5-10 minutes. Then, the reaction mixture was extracted into 20 mL of EtOAc and the catalyst was filtered off. After washing the filtrate with dil. HCl, Na₂CO₃, and brine solutions, pure products were eluted out by column chromatography using hexane-EtOAc (10:1). The main advantages of using MgO NPs are easy handling and cost effectiveness. Reaction was conducted at slightly lesser and higher amounts of catalyst to establish optimal yield, at room temperature. At 0.70 mmol of the catalyst good yields were obtained. Larger amount of catalyst (> 0.70 mmol) neither affected the yield nor the reaction rate. **Table 1** gives the optimized reaction conditions for preparation of *N*^α-protected selenoesters.

After optimizing the reaction conditions, this template was used for other *N*^α-protected amino acid chlorides to prepare selenoesters as shown in **Table 2**. The products were obtained in good yields and confirmed by FT-IR, ¹H NMR, ¹³C NMR and mass spectrometry.

3.2. Reusability of MgO NPs

To test the reusability of MgO NPs, a characteristic feature of heterogeneous catalysts, four consecutive experiments (1a) were conducted and the results are displayed in **Table 3**. After each experiment, the catalyst was washed with *n*-hexane and heated at 110°C in a hot air oven to remove the organic contaminants present in the catalyst surface. The MgO NPs show good catalytic activity with a yield of 84% up to the third cycle. After the third trial, the catalyst activity was decreased to the fourth run with a yield of 79%. Decreased catalytic activity could be due to the existence of organic contaminants on surface of the catalyst causing poisoning and pore filling.

Spectral data of the synthesized selenoesters (Table 2)

1. *N*^α-Fmoc-Val-CO-Se-GlyOMe (1a)

Yield 89%, Melting point 183 °C.

IR (KBr, cm^{-1}): 3433, 2081, 1624, 1212, 656. R_f (hexane-EtOAc, 9:1) = 0.3.

^1H NMR, (DMSO-d_6 , 400 MHz): δ 1.05-1.13 (d, J = 8.0 Hz, 6H), 2.15 (s, 2H), 2.51-2.68 (m, 1H), 3.60 (s, 3H), 4.30-4.63 (m, 4H), 6.60 (br, 1H), 7.10-7.80 (m, 8H) ppm.

^{13}C NMR, (DMSO-d_6 , 100 MHz): δ 14.70, 18.05, 32.31, 46.60, 51.57, 51.80, 62.97, 65.18, 125.19, 127.01, 127.25, 128.89, 140.68, 143.89, 155.13, 156.20, 174.09 ppm.

Mass calculated for $\text{C}_{23}\text{H}_{25}\text{NNaO}_5\text{Se}$: m/z 498.0796 ($\text{M} + \text{Na}^+$), found: 498.0797.

2. N^α -Fmoc-Cys-CO-Se-GlyOMe (1b)

Yield 75%, Melting point 159 °C

R_f (hexane-EtOAc, 9:1) = 0.3.

IR (KBr, cm^{-1}): 3450, 2092, 1640, 1220, 670.

^1H NMR, (CDCl_3 , 400 MHz): δ 1.6 (s, 1H), 2.5 (br, 2H), 3.0 (d, J = 6.0 Hz, 2H), 3.70 (s, 3H), 4.50-4.80 (m, 4H), 6.0 (br, 1H), 7.30-7.70 (m, 8H) ppm.

^{13}C NMR, (CDCl_3 , 100 MHz): δ 18.0, 28.0, 48.30, 53.0, 60.90, 68.70, 126.90, 128.20, 128.40, 128.80, 142.0, 143.80, 156.0, 171.0, 200.0 ppm.

Mass calculated for $\text{C}_{21}\text{H}_{21}\text{NO}_5$: m/z 502.0203 ($\text{M} + \text{Na}^+$), found: 502.0204.

3. N^α -Fmoc-Ala-CO-Se-LeuOMe (1c)

Yield 82%, Melting point 178 °C.

R_f (hexane-EtOAc, 9:1) = 0.3.

IR (KBr, cm^{-1}): 3428, 2090, 1655, 1230, 656.

^1H NMR, (CDCl_3 , 400 MHz): δ 0.88-0.90 (d, J = 8.0 Hz, 6H), 1.30-1.59 (m, 5H), 1.71-2.01 (m, 1H), 2.30-2.79 (t, J = 6.0 Hz, 1H), 3.79 (s, 3H), 4.08-4.64 (m, 4H), 6.58 (br, 1H), 7.20-7.80 (m, 8H) ppm.

^{13}C NMR, (CDCl_3 , 100 MHz): δ 17.93, 18.65, 20.99, 21.50, 21.55, 40.38, 41.40, 43.48, 44.30, 69.07, 124.94, 124.99, 127.03, 127.78, 141.33, 143.51, 143.56, 155.62 ppm.

Mass calculated for $\text{C}_{25}\text{H}_{29}\text{NO}_5\text{Se}$: m/z 526.1109 ($\text{M} + \text{Na}^+$), found: 526.1104.

4. N^α -Cbz-Met-CO-Se-TryOMe (1d)

Yield 76%, Melting point 159 °C.

R_f (hexane-EtOAc, 9:1) = 0.2.

IR (KBr, cm^{-1}): 3466, 2077, 1656, 1230, 680.

^1H NMR, (CDCl_3 , 400 MHz): δ 2.10 (s, 3H), 2.20-2.80 (m, 7H), 3.70 (s, 3H), 4.40 (m, 1H), 5.30 (s, 2H), 6.20 (br, 2H), 7.0-7.20 (m, 9H) ppm.

^{13}C NMR, (CDCl_3 , 100 MHz): δ 18.0, 26.0, 30.0, 32.10, 33.0, 52.0, 56.0, 66.0, 115.80, 127.20, 127.70, 129.0, 129.40, 132.0, 141.0, 155.50, 156.0, 172.20, 202.0 ppm.

Mass calculated for $\text{C}_{23}\text{H}_{27}\text{NO}_6\text{SSe}$: m/z 548.0622 ($\text{M} + \text{Na}^+$), found: 548.0623.

5. N^α -Fmoc-Tyr-CO-Se-ThrOMe (1e)

Yield 80%, Melting point 160 $^\circ\text{C}$,

R_f (hexane-EtOAc, 9:1) = 0.4.

IR (KBr, cm^{-1}): 3460, 2075, 1622, 1244, 658.

^1H NMR, (CDCl_3 , 400 MHz): δ 1.30 (d, J = 6.0, 3H), 2.4 (m, 2H), 3.0 (d, J = 8.0 Hz, 2H), 3.70 (s, 3H), 4.40-4.80 (m, 5H), 6.0 (br, 2H), 6.60-6.90 (m, 4H), 7.20-7.80 (m, 8H) ppm.

^{13}C NMR, (CDCl_3 , 100 MHz): δ 24.60, 38.0, 48.0, 52.0, 56.0, 59.0, 67.60, 116.0, 126.0, 128.20, 128.40, 128.80, 129.40, 132.0, 141.0, 143.60, 155.80, 156.0, 172.0, 201.0 ppm.

Mass calculated for $\text{C}_{29}\text{H}_{29}\text{NO}_7\text{Se}$: m/z 606.1007 ($\text{M} + \text{Na}^+$), found: 606.1457.

6. N^α -Fmoc-Leu-CO-Se-AlaOMe (1f)

Yield 87 %, Melting point 178 $^\circ\text{C}$,

R_f (hexane-EtOAc, 9:1) = 0.3.

IR (KBr, cm^{-1}): 3460, 2088, 1650, 1244, 690.

^1H NMR, (CDCl_3 , 400 MHz): δ 0.80-1.0 (d, J = 6.0 Hz, 6H), 1.20-1.30 (d, J = 12.0 Hz, 3H), 1.40-1.78 (m, 3H), 2.40-2.59 (m, 1H), 3.68 (s, 3H), 4.20-4.75 (m, 4H), 6.10 (br, 1H), 7.20-7.80 (m, 8H) ppm.

^{13}C NMR, (CDCl_3 , 100 MHz): δ 21.66, 21.78, 22.80, 24.73, 29.65, 41.39, 47.15, 52.34, 67.02, 124.90, 125.02, 127.02, 127.67, 141.28, 143.64, 143.83, 156.13, 177.77 ppm.

Mass calculated for $\text{C}_{25}\text{H}_{29}\text{NO}_5\text{Se}$: m/z 526.1109 [$\text{M} + \text{Na}$] $^+$, found: 526.1179.

7. N^α -Fmoc-Phe-CO-Se-AlaOMe (1g)

Yield 80 %, Melting point 176 $^\circ\text{C}$.

R_f (Hexane-EtOAc, 9:1) = 0.3.

IR (KBr, cm^{-1}): 3460, 2088, 1674, 1248, 678.

^1H NMR, (CDCl_3 , 400 MHz): δ 1.25-1.28 (d, J = 4.0 Hz, 3H), 2.50-2.69 (q, J = 2.5 Hz, 1H), 2.89-2.99 (d, J = 2.9 Hz, 2H), 3.88 (s, 3H), 4.02-4.49 (m, 4H), 6.10 (br, 1H), 7.26-7.34 (m, 13H) ppm.

^{13}C NMR, (CDCl_3 , 100 MHz): δ 15.33, 31.78, 31.96, 34.70, 53.38, 60.71, 77.31, 127.37, 128.06, 128.16, 128.22, 128.48, 128.60, 128.71, 136.10, 141.63, 155.80, 156.01, 171.76, 174.75 ppm.

Mass calculated for $\text{C}_{28}\text{H}_{27}\text{NO}_5\text{Se}$: m/z 560.0952 $[\text{M}+\text{Na}]^+$, found: 560.0955.

8. N^α -Fmoc-Ala-CO-Se-TyrOMe (1h)

Yield 78%, Melting point 178 °C.

R_f (Hexane-EtOAc, 9:1) = 0.3.

IR (KBr, cm^{-1}): 3460, 2088, 1650, 1240, 692.

^1H NMR (CDCl_3 , 400 MHz): δ 1.41 (d, J = 6.0 Hz, 3H), 2.80 (m, 3H), 3.70 (s, 3H), 4.45-4.70 (m, 4H), 6.20 (br, 2H), 7.0-7.90 (m, 12H) ppm.

^{13}C NMR (CDCl_3 , 100 MHz): δ 18.0, 26.0, 34.0, 47.0, 52.0, 54.0, 66.40, 115.40, 126.8, 128.20, 128.60, 128.80, 130.0, 132.10, 141.0, 143.60, 155.70, 156.0, 172.20, 202.0 ppm.

Mass calculated for $\text{C}_{28}\text{H}_{27}\text{NO}_6\text{Se}$: m/z 576.0901 $[\text{M}+\text{Na}]^+$, found: 576.0904.

3.3. Antifungal activity of studies

Antifungal activity of the synthesized selenoesters against *F. oxysporum* and *A. niger* have been summarized in **Tables 4** and **5**. From the data, it is clear that the compounds such as N^α -Fmoc-Cys-CO-Se-GlyOMe (1b), N^α -Fmoc-Tyr-CO-Se-ThrOMe (1e), and N^α -Fmoc-Ala-CO-Se-TyrOMe (1h) possess high activity, and the compounds N^α -Fmoc-Val-CO-Se-GlyOMe (1a), N^α -Fmoc-Ala-CO-Se-LeuOMe (1c), N^α -Cbz-Met-CO-Se-TyrOMe (1d), N^α -Fmoc-Leu-CO-Se-AlaOMe (1f), and N^α -Fmoc-Phe-CO-Se-AlaOMe (1g) possess moderate activity against *F. oxysporum* strains. Whereas, *A. niger* strain exhibited moderate zones of inhibition for the N^α -Fmoc-Cys-CO-Se-GlyOMe (1b), N^α -Fmoc-Ala-CO-Se-LeuOMe (1c), N^α -Fmoc-Tyr-CO-Se-ThrOMe (1e), N^α -Fmoc-Leu-CO-Se-AlaOMe (1f), and N^α -Fmoc-Ala-CO-Se-TyrOMe (1h), the N^α -Cbz- of inhibition. The maximum zone of inhibition was observed for the N^α -Fmoc-Val-CO-Se-GlyOMe (1a) against *A. niger*. Overall, the protected selenoesters

showed significant values of zones of inhibition.

3.4. Study of properties of biodiesel

Properties of biodiesel evaluated as per the ASTM standards are tabulated in **Table 6**. Viscosity and density of biodiesel are observed to be 5.4cSt and 880 kg/m³ respectively. The biodiesel flash point is 165 °C and is in the standard range, and the value is also safer for handling and utilization of produced fuel. Copper strip corrosion test (ASTM D130) was conducted, and the value was found to be 1a and lies within accepted range. The acid value was 0.2 Mg KOH/g. Therefore, the results of this work showed that MgO NPs have appreciable catalytic activity for biodiesel production. Results of all the parameters of biodiesel are well within the standard range of ASTM standards, comparable with that of the normal diesel, and hence the biodiesel is suitable for use in CI engine as a fuel.

Conclusions

In conclusion, an efficient synthesis of MgO NPs *via* solution combustion method using aqueous plant extract of *Terminalia chebula* seeds, characterization of MgO NPs and the catalytic property have been demonstrated in this study. FTIR spectra indicates the stretching bond corresponding to Mg-O at 440 cm⁻¹, and hydroxyl group at 3435 cm⁻¹. XRD results showed that the average crystallite size of MgO NPs was measured as 32.76 nm. EDAX confirms that the % of Mg and O element in MgO NPs is 42.85 and 56.26. The catalytic activity of MgO NPs for organic transformations was established by the solution phase preparation of selenoesters. The Selenoesters obtained were characterized by spectral methods such as mass spectrometry, ¹H NMR, ¹³C NMR, and FTIR. The protocol for the synthesis of selenoesters has merits of milder reaction conditions, easy work-up procedure and higher product yields. The antifungal activities of the synthesized selenoesters indicate that *N*^α-Fmoc-Ala-CO-Se-TyrOMe shows activity against *A. niger* giving us a scope for further pharmacological investigation. Recycling of the cooking oil for the production of biodiesel not only confirms the catalytic performance of MgO NPs but can also be explored for upgrading for large scale production which can be used in CI engines as fuel.

Acknowledgement

The authors thank the Principal, CEO and Director of Siddaganga Institute of Technology, Tumakuru, Karnataka, India for providing research facilities. We also thank Research and Development Lab, Chemistry Department and Bioenergy Research Information & Demonstration Centre(BRIDC),SIT, Tumakuru for providing necessary experimental setup to perform this research work.

Conflict of interest

The authors declare there is no conflict of interest in carrying out this research work.

References

1. A. Annu, R. Ali, J. Gadkari, S. Sheikh, Ahmed, A. Husen, M. Iqbal (eds.), *Nanomaterials and Plant Potential*, **2019**, pp. 261–284. https://doi.org/10.1007/978-3-030-05569-1_10.
2. J. P. Singh, V. Singh, A. Sharma, G. Pandey, K. H. Chae, S. Lee, *Heliyon*, **2020**, *6*, 1–14. <https://doi.org/10.1016/j.heliyon.2020.e04882>.
3. H. M. Fahmy, M. H. El-Hakim, D. S. Nady, Y. Elkaramany, F. A. Mohamed, A. M. Yasien, M. A. Moustafa, B. E. Elmsery, H. A. Yousef, *Nanomed. J.* **2022**, *9(1)*, 1–14. <https://doi.org/10.22038/NMJ.2021.60646.1629>.
4. Yunhui Bao, Jian He, Ke Song, Jie Guo, Xianwu Zhou, and Shima Liu, *Hindawi J. Chem.* **2021**, <https://doi.org/10.1155/2021/6562687>.
5. Adeyemi, J.O.; Oriola, A.O.; Onwudiwe, D.C.; Oyediji, A.O. Plant Extracts Mediated Metal-Based Nanoparticles: Synthesis and Biological Applications. *Biomolecules*, **2022**, *12*, 627. <https://doi.org/10.3390/biom12050627>.
6. S. T. Fardood, A. Ali Ramazani, S. W. Joo, *J. App. Chem. Res.*, **2017**, *11*, 8–17. <https://doi.org/10.33945/SAMI/CHEMM.2019.5.1>.
7. A. Verma, M. S. Mehtha, *J. Rad. Res. App. Sci.*, **2016**, *9*, 109–11.
8. J. Balavijayalakshmi, V. Ramalakshmi, *J. App. Res. Technol.*, **2017**, *15*, 413–422. <https://doi.org/10.1016/j.jart.2017.03.010>.
9. N. Jayaprakash, J. J. Vijaya, K. Kaviyarasu, K. Kombaiah, L. J. Kennedy, R. J. Ramalingam, Murugan A. Munusamy, Hamad A. Al-Lohedan, *J. Photochem. Photobiol. B, Biol.*, **2017**, *169*, 178–185. <https://doi.org/10.1016/j.jphotobiol.2017.03.013>
10. de la Rosa, Guadalupe, López-Moreno, M. Laura, de Haro, David, Botez, E. Cristian, Peralta-Videa, R. José, Gardea-Torresdey, L. Jorge, *Pure Appl. Chem.*, **2013**, *85*, 2161–2174. <https://doi.org/10.1351/PAC-CON-12-09-05>.
11. H. Dabhane, Ghotekar, P. Tambade, S. Pansambal, R. Oza, V. Medhane, *Eur. J. Chem.* **2021**, *12 (1)*, 86–108. <https://doi.org/10.5155/eurjchem.12.1.86-108.2060>.
12. I. Khan, Z. Ullah, A. A. Shad, M. Fahim, M. Öztürk, *South Afri. J. Bot.*, **2022**, *146*, 395–400. <https://doi.org/10.1016/j.sajb.2021.11.016>.

13. H. S. Lalithamba, M. Raghavendra, K.V. Yatish, *J. Electron. Mater.* **2022**, *51*, 3650–3659.
<https://doi.org/10.1007/s11664-022-09610-x>
14. Antonyak H., Iskra R., Panas N., and Lysiuk R., Selenium. In: Malavolta M., Mocchegiani E. (eds) Trace Elements and Minerals in Health and Longevity, Healthy Ageing and Longevity, *Springer*, 8, 2018, 63–98.
15. S. J. Fairweather-Tait, Y. Bao, M. R. Broadley, R. Collings, D. Ford, J. E. Hesketh, R. Hurst, *Antioxid. Redox Signal.* **2011**, *14*, 1337–1383. <https://doi.org/10.1007/s12263-011-0256-4>.
16. J. Kohrle, B. R. Flohe, A. Bock, R. Gartner, O. Meyer, O. Fohle, *Biol. Chem. J.*, **2000**, *381*, 849–864.
17. S. Hariharan, S. Dharmaraj, *Inflammopharm.*, **2020**, *28(3)*, 667–695.
<https://doi.org/10.1007/s10787-020-00690-x>.
18. N. T. T. Huong, K. Matsumoto, R. Kasai, K. Yamasaki, W. Watanabe, *Bio. Pharm. Bull.*, **1998**, *21*, 978. doi : <https://doi.org/10.1248/cpb.51.1413>.
19. C. Lowig, *J. Pogg. Ann.*, **1836**, *37*, 552.
20. T. Kataoka, S. Watanabe, Alkyl Chalcogenides: Selenium- and Tellurium-based Functional Groups, Ed (s): Alan R. Katritzky, Richard J.K. Taylor, Comprehensive Organic Functional Group Transformations II, Elsevier, pp. 237–254.
21. M. Álvarez-Pérez, W. Ali, M. A. Marć, J. Handzlik, E. Domínguez-Álvarez, *Molecules*. **2018**, *23(3)*, 628–638. <https://doi.org/10.3390/molecules23030628>.
22. S. Shaaban, A. M. Ashmawy, A. Negm, L. A. Wessjohann. *Eur. J Med. Chem.* **2019**, *179*, 515–526. <https://doi.org/10.1016/j.ejmech.2019.06.075>.
23. D. Radomska, R. Czarnomysy, A. Szymanowska, D. Radomski, E. Domínguez-Álvarez, A. Bielawska, K. Bielawski. *Cancers (Basel)*. **2022**, *14(17)*, 4304.
<https://doi.org/10.3390/14174304>.
24. J. B. Rocha, B. Piccoli, C. S. Oliveira, J. Joule, *Arkivoc*, **2017**, *2017*, 457–491.
<https://doi.org/10.24820/ark.5550190.p009.784>.
25. Z. Chen, H. Lai, L. Hou, T. Chen, *Chem. Commun.* **2020**, *56*, 179–196.
<https://doi.org/10.1039/C9CC07683B>.
26. J. Ramanujam, U. P. Singh, *J. Energy Environ. Sc.* **2017**, *6*.
<https://doi.org/10.1039/C7EE00826K>

26. T. Tang, Copper Indium Gallium Selenide Thin Film Solar Cells, Ed. Narottam Das, *Nanostructured Solar Cells*, **2017**, <https://doi.org/10.5772/65291>.
27. L. B. Antonio, J. N. S. Sandra, S. L. Diogo, L. D. Roberta, C. S. Claudio, B. T. Joao, L. Rochaa, A. Wessjohann, *Tet. Lett.*, **2002**, 43, 7329–7331. [https://doi.org/10.1016/S0040-4039\(02\)01713-6](https://doi.org/10.1016/S0040-4039(02)01713-6).
28. L. B. Antonio, V. Fabrício, A. S. Jasquer, C. B. Rodolpho, *J. Org. Chem.*, **2005**, 70, 9021–9024. <https://doi.org/10.1021/jo051451a>
29. N. Yoshiaki, S. Kyohei, J. D. Singh, F. Shin-ichi, O. Kouichi, U. Sakae, *Organometallics*, **1996**, 15, 370–379. <https://doi.org/10.1021/om950533u>.
30. D. S. Rampon, F. S. Rodembusch, P. F. B. Gonçalves, R. V. Lourega, A. A. Merlo, P. H. Schneider, *J. Braz. Chem. Soc.*, **2010**, 21, 2100–2107. <https://doi.org/10.1590/S0103-50532010001100011>.
31. T. Durek, P.F. Alewood. *Angew. Chem. Int. Ed. Eng.*, **2011**, 50, 12042–12045. <https://doi.org/10.1002/anie.201105512>.
32. M.-L. Bennasar, E. Zulaica, D. Solé, T. Roca, D. García-Díaz, S. Alonso. *J. Org. Chem.*, **2009**, 74, 8359–8368. <https://doi.org/10.1021/jo901986v>.
33. F. N. Victoria, D. M. Martinez, M. Castro, A. M. Casaril, D. Alves, E. J. Lenardão, H. D. Salles, P. H. Schneider, L. Savegnago, *Chem. Biol. Interact.* **2013**, 205, 100–107. <https://doi.org/10.1016/j.cbi.2013.06.019>.
34. C. Sanmartín, D. Plano, E. Domínguez, M. Font, A. Calvo, C. Prior, I. Encío, J. A. Palop, *Molecules*, **2009**, 14, 3313–3338. <https://doi.org/10.3390/molecules14093313>.
35. E. Domínguez-Álvarez, D. Plano, M. Font, A. Calvo, C. Prior, C. Jacob, J. A. Palop, C. Sanmartín. *Eur. J. Med. Chem.* **2014**, 73, 153–166. <https://doi.org/10.1016/j.ejmech.2013.11.034>.
36. A. Makriyannis, W. H. H. Guenther, H. G. Mautner, *J. Am. Chem. Soc.* **1973**, 95, 8403–8406.
37. W. A. Reinerth, J. M. Tour, *J. Org. Chem.* **1998**, 63, 2397–2400.
38. A. F. Sviridov, M. S. Ermolenko, D. V. Yashunskii, N. K. Kochetkov, *Bull. Acad. Sci. USSR Div. Chem. Sci.* **1985**, 34, 1514–1518.
39. H. Rikiishi, *J. Bioenerg. Biomembranes*, **2007**, 39, 91–98. <https://doi.org/10.1007/s10863-006-9065-7>.

40. M. L. Smith, J. K. Lancia, T. I., Mercer Ip C, *Anticancer Research*, **2004**, 24, 1401–1408.
41. M. Godoi, E. Ricardo, G. Botteselle, F. Galetto, J. Azeredo, A. Braga. *Green Chem.*, **2012**, 14, 456–460. <https://doi:10.1039/C1GC16243H>.
42. T. Inoue, T. Takeda, N. Kambe, A. Ogawa, I. Ryu, N. Sonoda, *J. Org. Che.*, **1994**, 59, 5824–5827.
43. S. I. Fujiwara, A. Asai, T. Shin-ike, N. Kambe, Noboru S., *J. Org. Chem.*, **1998**, 63, 1724–1726.
44. C. C. Silveira, A. L. Braga, E. L. Larghi, *Organometallics*, **1999**, 18, 5183–5186. <https://doi.org/10.1021/om990589e>.
45. C. Rana, M. Anindita, S. Sougata, V. Z. Grigory, M. Adinath, *Tetrahedron*, **2019**, 75, 130624. <https://doi.org/10.1016/j.tet.2019.130624>.
46. B. Gemma, S. Marialaura, P. V. Jaqueline, S. Luca, B. Luana, M. Francesca, S. L. Diogo, J. L. Eder, S. Claudio, *J. Chem.*, **2016**, 1–8.
47. A. Temperini, F. Piazzolla, L. Minuti, M. Curini, C. Siciliano, *J. Org. Chem.* **2017**, 82, 4588–4603. <https://doi.org/10.1021/acs.joc.7b00173>.
48. S. Specchia, C. Galletti, V. Specchia, Solution Combustion Synthesis as intriguing technique to quickly produce performing catalysts for specific applications, Editor(s): E.M. Gaigneaux, M. Devillers, S. Hermans, P.A. Jacobs, J.A. Martens, P. Ruiz, *Studies in Surface Science and Catalysis*, Elsevier, 175, 2010, 59–67.
49. K.V. Rao, C. S. Sunandana, *J. Mater. Sci.* 43, **2008**, 146–154, <https://doi.org/10.1007/s10853-007-2131-7>.
50. K. Kaviyarasu, P. A. Devarajan, *Der Pharma Chemica*, **2011**, 3(5), 248–254.
51. Q. Dengfeng, Z. Liangping, Z. Dengbo, C. Yufeng, G. Zhufen, F. Renjun, Z. Miaoyi, Kan L., X. Jianghui., W. Wei., *Front. Microbiol.*, **2019**, 10(1390), 1–15. <https://doi.org/10.3389/fmicb.2019.01390>.
52. W. R. Li, Q. S. Shi, Y. S. Ouyang, Y. B. Chen, S. S. Duan, *App. Microbiol. Biotechnol.*, **2013**, 97(16), 7483–7492. <https://doi:10.1007/s00253-012-4460-y>.
53. T. D. Khodair, H. A. Abed, G. S. Majeed. *Int. J. Sci. Eng. Technol.*, **2016**, 3, 2400–2406. <https://doi:10.1038/s41598-018-22134-x>.

Scheme 1: Methods of preparation of selenolesters

Figure 1. XRD Pattern of MgO

Figure 2. FT-IR spectrum of the MgO NPs

Figure 3. SEM images of MgO NPs at different resolutions; a) 900X, b) 400X

Figure 4. EDAX spectrum of MgO NPs

Figure 5. TEM images of MgO NPs at different magnifications; a) 100 kX, b) 50 kX

6. a) Diffuse reflectance spectrum of MgO NPs. b) Direct band gap energy of MgO NPs

Table 1: Optimized reaction conditions for preparation of N^{α} -protected selenoesters

Scheme 2: Synthesis of selenoesters derivatives

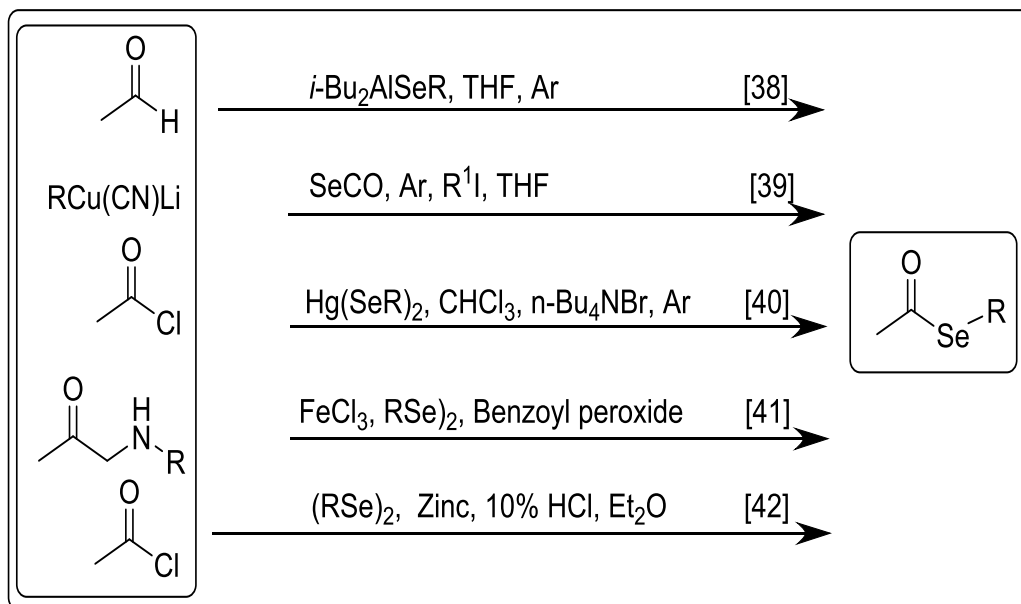
Table 2: Synthesized N^{α} -protected selenoesters derivatives (Scheme 2)

Table 3: Reusability of MgO NPs

Table 4: Antifungal activity of selenoesters against *F. oxysporum*

Table 5: Antifungal activity of selenoesters against *A. niger*

Table 6: Properties of the biodiesel fuel



Scheme 1: Methods of preparation of selenolesters

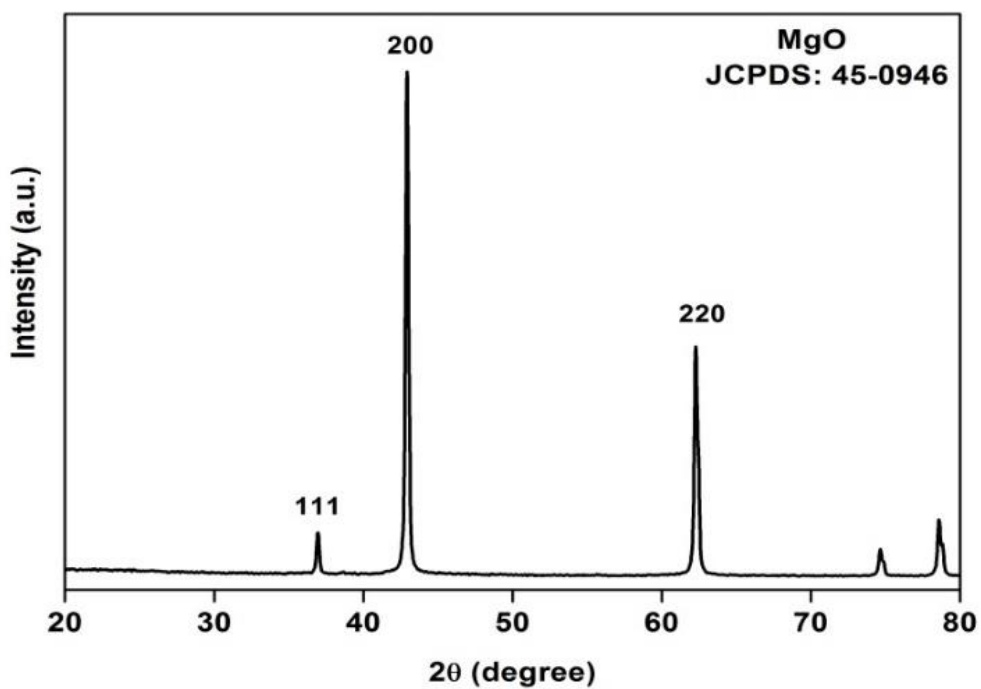


Figure 1. XRD Pattern of MgO

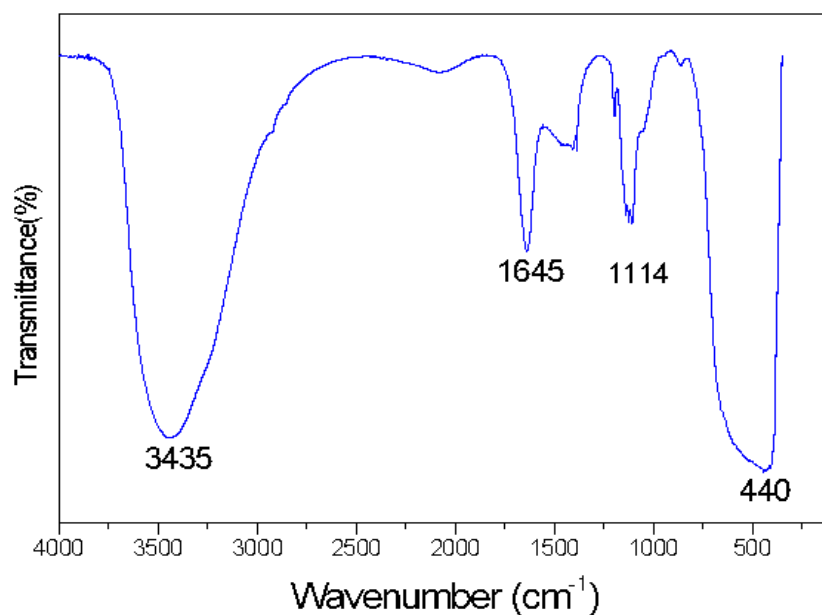


Figure 2. FT-IR spectrum of the MgO NPs

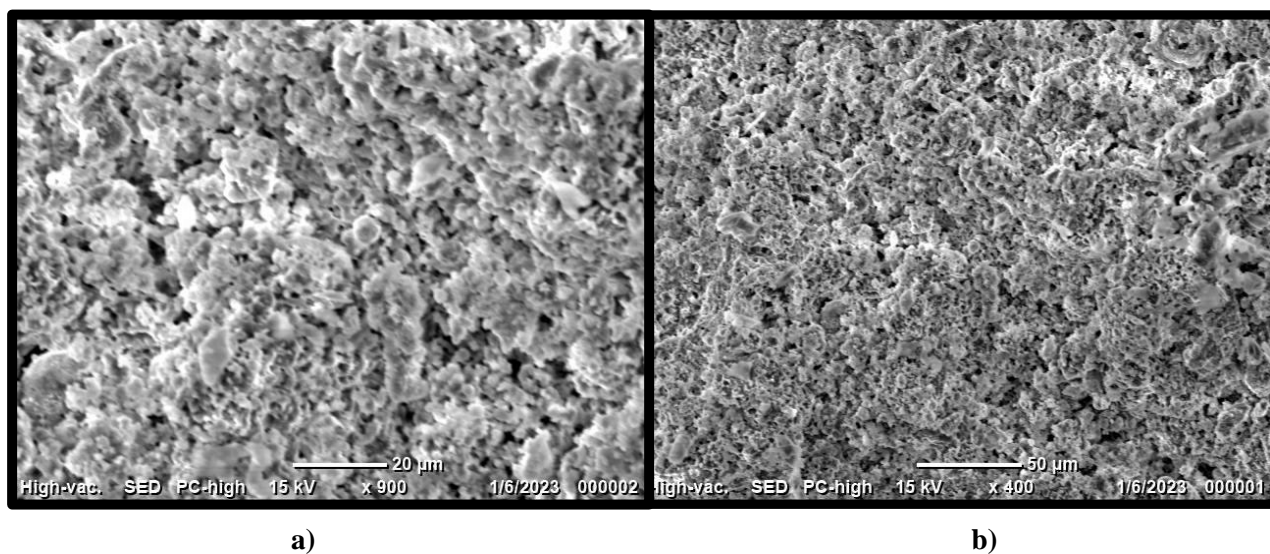


Figure 3. SEM images of MgO NPs at different resolutions; a) 900X, b) 400X

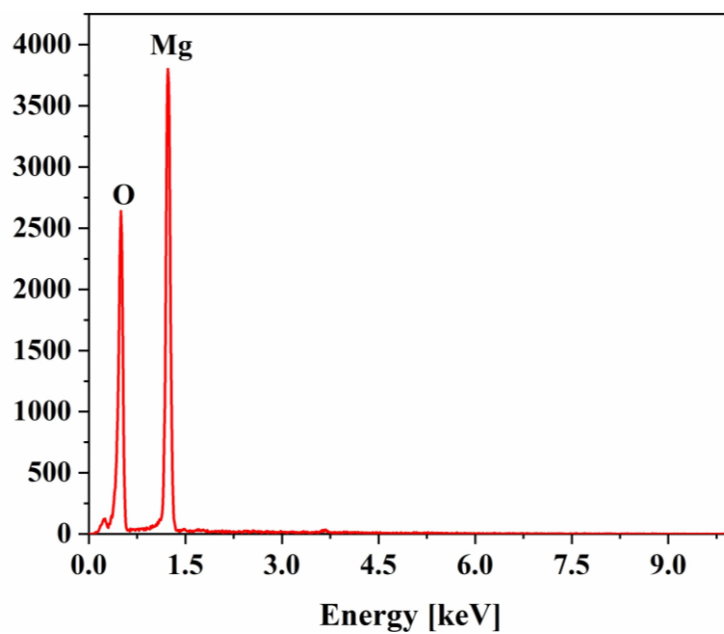


Figure 4. EDAX spectrum of MgO NPs

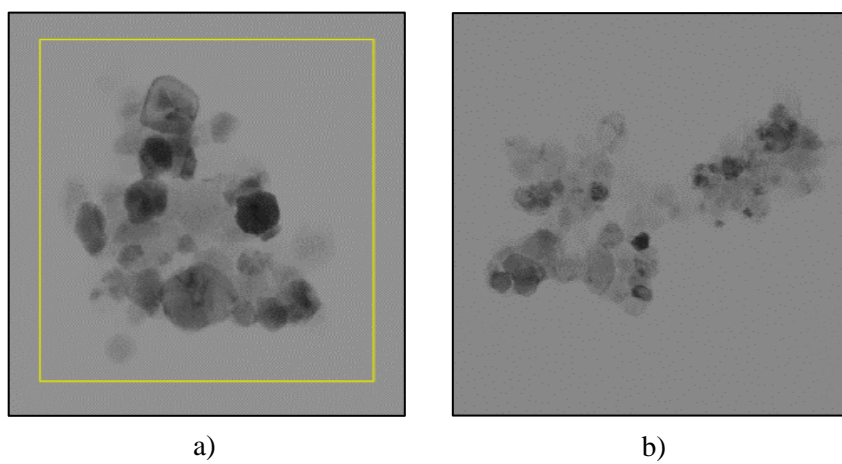


Figure 5. TEM images of MgO NPs at different magnifications; a) 100 kX, b) 50 kX

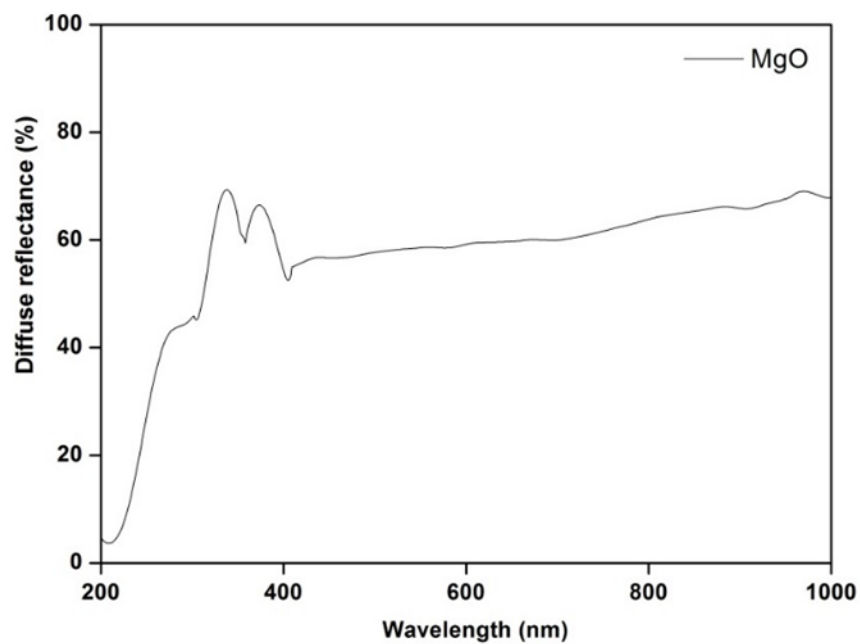


Figure 6. a) Diffuse reflectance spectrum of MgO NPs.

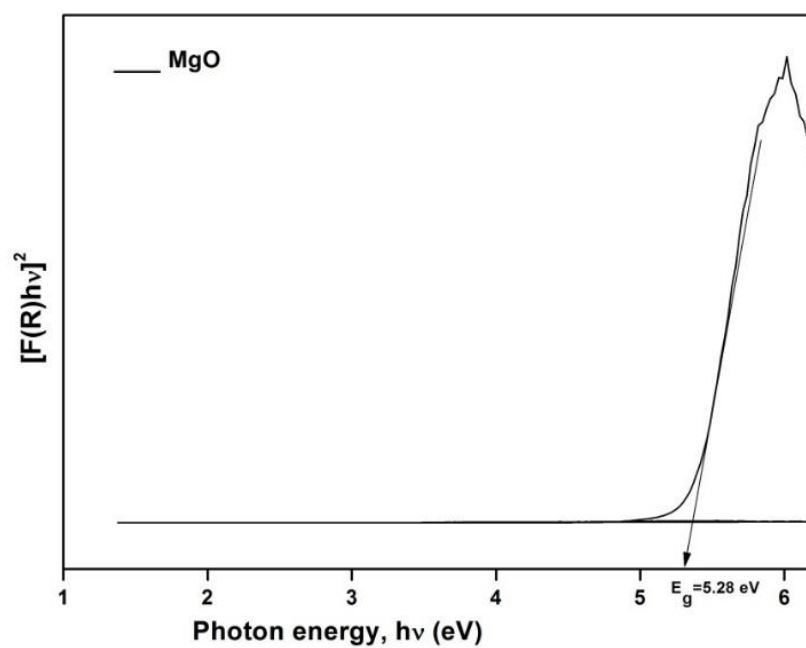
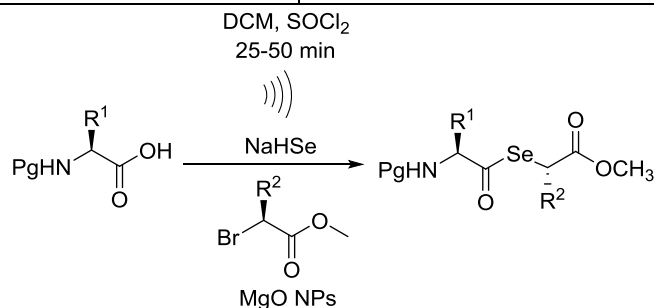


Figure 6. b) Direct band gap energy of MgO NPs

Table 1: Optimized reaction conditions for preparation of N^α -protected selenoesters

Conditions	Optimized Parameters
Catalyst	MgO NPs
Temperature	Room Temperature
Solvent	Ethyl acetate
Catalyst concentration	0.70 mmol
Time	8-10 hours



Scheme 2: Synthesis of selenoester derivatives

Table 2: Synthesized N^α -protected selenoester derivatives (Scheme 2)

Entry	N^α -protected selenoesters	Yield (%)	Mp (°C)
1a		89	178
1b		75	159
1c		82	178
1d		76	156

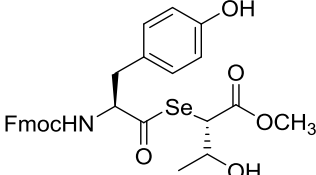
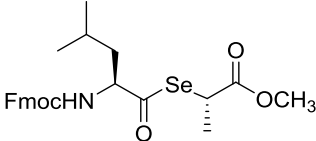
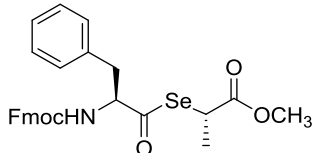
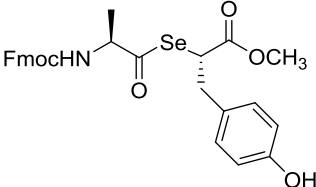
1e		80	160
1f		87	178
1g		80	176
1h		78	178

Table 3: Reusability of MgO NPs

Reusability	% Yield
1 st time	89
2 nd time	86
3 rd time	84
4 th time	79

Table 4: Antifungal activity of selenoesters against *F. oxysporum*

Entry	Treatment (Concentration in μg/μL)	<i>F.oxysporum</i> (Mean±SE)
Standard Fluconazole	25	72.00 ± 0.04
1a	100	41.20 ± 0.06
1b	100	39.11 ± 0.06
1c	100	53.24 ± 0.07
1d	100	38.08 ± 0.08

1e	100	42.39 ± 0.10
1f	100	54.37 ± 0.10
1g	100	53.33 ± 0.12
1h	100	34.56 ± 0.13

Table 5: Antifungal activity of selenoesters against *A. niger*

Entry	Treatment (Concentration in µg/µL)	<i>A. niger</i> (Mean±SE)
Standard Fluconazole	25	70.00 ± 0.04
1a	100	65.27 ± 0.20
1b	100	9.57 ± 0.15
1c	100	53.61 ± 0.15
1d	100	69.26 ± 0.15
1e	100	28.64 ± 0.12
1f	100	69.00 ± 0.04
1g	100	32.63 ± 0.10
1h	100	76.67 ± 0.14

Table 6: Properties of the biodiesel fuel

Sl. No.	Properties	ASTM standard	ASTM Range	Normal Diesel	Biodiesel produced using synthesized MgO NPs
1	Density at 15 °C (kg/m ³)	D4052	860-900	834	880
2	Viscosity at 40 °C (cSt)	D445	1.9-6.0	2.6	5.4
3	Flash point (°C)	D93A	>130	60	165
4	Copper strip corrosion, 50 °C, 2h	D130	no.3 max	1a	1a
5	Acid value (mg KOH/g)	D664	0.50 max	0.20	0.2

Biographies

H S Lalithamba was born in India in 1973. She received her BSc and MSc degrees in Chemistry and Organic Chemistry from Bangalore University, Bangalore, India in 1994 and 1996, respectively. Also, she received a PhD degree in Peptides and Peptidomimetics from the same university in 2012. She is currently an Associate Professor at the Department of Chemistry, Siddaganga institute of Technology, Tumakuru, India. Her research interests include synthesis of biologically active peptides and peptidomimetics, biological activity, molecular docking, and nanometal oxides. She actively contributed to funded projects of VGST, Government of Karnataka on the synthesis of bioactive peptides and peptidomimetics research. She has published more than 35 scientific research articles in well-known journals.

Omkaresh B R was born in India in 1990. He received his B.E. and M.Tech degree in Mechanical Engineering and Thermal power engineering from VTU, Belagavi respectively. He received Ph.D. degree from the University of VTU, Belagavi in the area Biodiesel. Currently he is working as assistant professor in the Department of Mechanical Engineering, Siddaganga institute of Technology, Tumakuru, India. Research work includes synthesis of biodiesel, characterization of biodiesel, CI Engine, catalyst synthesis. He also worked and contributed to funded projects by VGST, KSCST and Karnataka State Bioenergy Development Board, Government of Karnataka. He published more than 15 scientific research articles in well-known journals.

Aisha Siddekha is presently working as Associate professor in the department of Chemistry, Government First Grade College, Tumkur, affiliated to Tumkur University, Karnataka, India. She has M.Sc. degree in Organic Chemistry (1996) from Bangalore University, and M.Phil. (2009) from Madurai Kamraj University, Madurai, India. She received the Ph.D. degree in the year 2018 in Green chemistry from Bangalore University. Her main research interests include synthesis of biologically active organic compounds, green chemistry, corrosion inhibition, vibrational studies, and nano metal oxides.

Anasuya K V was born in India in 1975. She received her bachelor's degree from Bangalore University in 1995 and M.Sc. degree in Inorganic Chemistry from Bangalore University,

Bangalore, India, in 1997 with Two Gold Medals for securing the highest marks in Inorganic Chemistry. She received the Ph.D. degree in Polymer Chemistry from Visvesvaraya Technological University, Belgaum in 2016. Currently she is working as Associate Professor in the Department of Chemistry, Government First Grade College, Tumakuru, Karnataka, India. Her research interests include synthesis and characterization of polymer-metal complexes. She has published more than 15 scientific research articles in well-known journals.